JOURNAL OF NATURAL PRODUCTS

Article

Cite This: J. Nat. Prod. XXXX, XXX, XXX−XXX

pubs.acs.org/jnp

Chemical Constituents of *Anneslea fragrans* and Their Antiausterity Activity against the PANC-1 Human Pancreatic Cancer Cell Line

Ashraf M. Omar,[†] Dya Fita Dibwe,[†] Ahmed M. Tawila,[†] Sijia Sun,[†] Ampai Phrutivorapongkul,[‡] and Suresh Awale*[,†]

[†]Division of Natural Drug Discovery, Institute of Natural Medicine, University of Toyama, 2630 Sugitani, Toyama 930-0194, Japan

[‡]Faculty of Pharmacy, Chiang Mai University, Chiang Mai 50200, Thailand

Supporting Information

ABSTRACT: An ethanolic extract of *Anneslea fragrans* leaves showed potent preferential cytotoxicity against PANC-1 human pancreatic cancer cells under a nutrient-deprived condition, with a PC_{50} value of 9.6 μg/mL. Phytochemical investigation of this active extract led to the isolation of two new secondary metabolites, fragranones A (**1**) and B (**2**), along with 15 previously reported compounds. The structure elucidation of the new compounds was achieved by HRFABMS, acid hydrolysis, NMR, and ECD spectroscopic analysis. Fragranone A (**1**) is the first example of a rare natural product bearing an acetonide glucose moiety. Fragranone B (**2**) is representative of a rare class of natural products with a threonolactone unit linked to a chalcone through an ether linkage. The isolated compounds exhibited antiausterity activity against PANC-1 cells under nutrient-deprived conditions, and betulin (**14**) was found to be the most potent compound tested, with a PC_{50} value of 8.4 μM. In addition, fragranone A (**1**) was found to suppress PANC-1 cancer cell migration in real time.

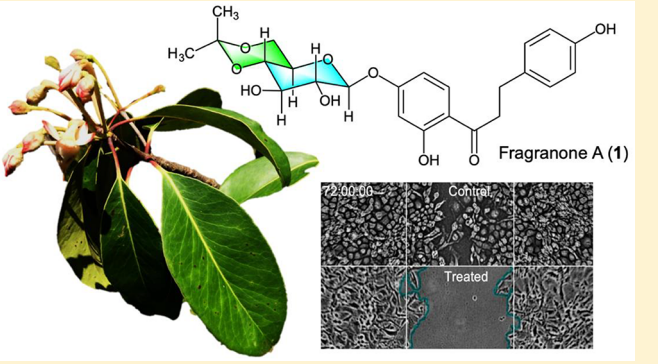

Cancer is continuing to be a challenging health problem in the 21st century. It was responsible for over 9.6 million deaths worldwide in the year 2018.[1] Among all types of cancer, pancreatic cancer is known to be the deadliest in having the lowest chance of survival after initial diagnosis. It has the lowest five-year relative survival rate of less than 5%.[2] In Japan, an estimated 40 000 patients were diagnosed with pancreatic cancer in 2018 and 34 900 deaths occurred from this malignancy.[2] The incidence rate is nearly equivalent to the mortality rate. The aggressiveness of pancreatic cancer and its inadequate response to either chemotherapy or radiotherapy have been complicated considerably due to both the absence of appropriate screening tests and diagnostic markers for its early detection.[3] Therefore, there is an urgent need to find effective new agents for the treatment of pancreatic cancer.

Pancreatic tumors are hypovascular in nature, yet they thrive under a nutrient-deficient "austere" tumor microenvironment. In particular, PANC-1 human pancreatic cancer cells have shown extreme tolerance to nutrition starvation and survive for a prolonged time even in the complete absence of glucose, amino acids, and serum.[4] Such a phenomenon is referred to as "austerity". An antiausterity strategy is an approach for discovering unique anticancer agents that can target preferentially the ability of cancer cells to tolerate nutritional starvation. Test compounds and extracts are evaluated under both nutrient-rich and nutrient-deprived conditions, and the agents showing preferential cytotoxicity against nutrient-deprived cancer cells without toxicity in nutrient-rich conditions are classified as "antiausterity agents".[4,5] Previous studies using this strategy resulted in the discovery of several potent antiausterity agents such as arctigenin,[4] angelmarin,[6] isopanduratin A1,[7] nicolaioidesin C,[7] bergamotin,[8] and ancistrolikokine E_3.[9]

In a continuing investigation, a 95% ethanolic extract of *Anneslea fragrans* Wall. (Theaceae) leaves, collected from the Chiang Mai Province of Thailand, showed discernible preferential cytotoxicity against PANC-1 cancer cells under a nutrient-deprived condition with a PC_{50} value of 9.6 μg/mL. Therefore, a phytochemical investigation of this active extract was carried out and resulted in the isolation of the new dihydrochalcone glucoside fragranone A (**1**) and the new chalcone fragranone B (**2**), together with 15 previously reported compounds. The isolated compounds can be classified as five dihydrochalcones, two chalcones, five flavonol 3-*O*-glycosides, three triterpenoids, and two miscellaneous compounds. The previously reported compounds were identified as 3,4,2′,4′-tetrahydroxydihydrochalcone (**3**),[10] confusoside (**4**),[11] vacciniifolin (**5**),[12] davidioside (**6**),[13] butein (**7**),[14] afzelin (**8**),[15] quercitrin (**9**),[16] isoquercitrin (**10**),[17] kaempferol 3-neohesperidoside (**11**),[18] nictoflorin (**12**),[19] lupeol (**13**),[20] betulin (**14**),[20] spinasterol (**15**),[21] (epi)catechin (**16**),[22] and isoscopoletin (**17**) (Chart 1).[23]

Received: August 2, 2019

DOI: 10.1021/acs.jnatprod.9b00735
J. Nat. Prod. XXXX, XXX, XXX−XXX

Chart 1

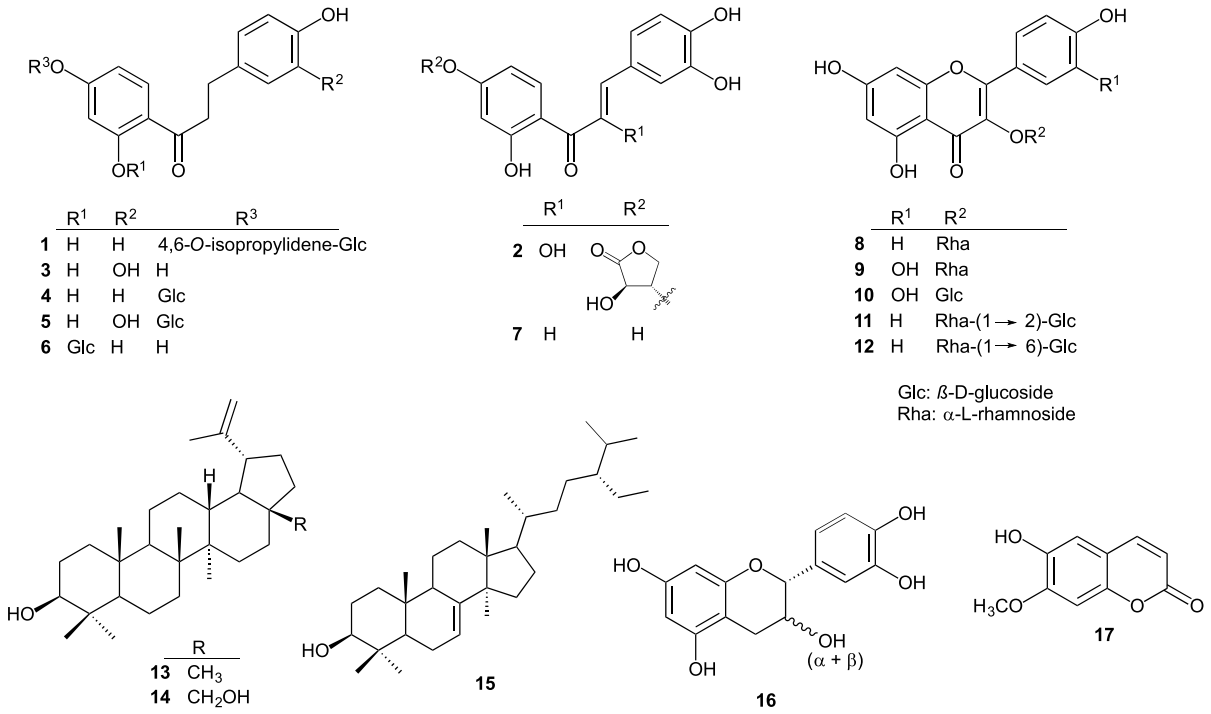

RESULTS AND DISCUSSION

Fragranone A (**1**) was isolated as a white, amorphous solid. Its molecular formula was deduced by HRFABMS as $C_{24}H_{28}O_9$ [*m*/*z* 461.18126 (M + H)$^+$]. The IR spectrum of **1** showed absorption bands for hydroxy (3420 cm^{-1}) and *α*,*β*-unsaturated carbonyl (1634 cm^{-1}) groups. The UV spectrum of **1** showed absorption maxima at 208, 272, and 320 nm. The ^{1}H NMR spectrum of **1** (Table 1) displayed the presence of a 1,4-disubstituted phenyl ring [δ_H 6.70 (d, *J* = 8.5 Hz, H-3,5) and 7.06 (d, *J* = 8.5 Hz, H-2,6)] along with signals for a 1,2,4-trisubstituted phenyl ring [δ_H 6.56 (d, *J* = 2.4 Hz, H-3′), 6.59 (dd, *J* = 2.4, 9.2 Hz, H-5′), and 7.81 (d, *J* = 9.2 Hz, H-6′)] and two mutually coupled methylenes [δ_H 2.92 (t, *J* = 7.6 Hz, H$_2$-*β*) and 3.23 (t, *J* = 7.6 Hz, H$_2$-*α*)]. These signals closely resembled those of davidigenin.[24] In addition, the ^{1}H NMR spectrum showed the presence of an anomeric proton [δ_H 5.09 (d, *J* = 7.3 Hz, H-1″)] and two diastereotopic protons [δ_H 3.78 (dd, *J* = 10.4, 10.5 Hz, H-6″b) and 3.91 (dd, *J* = 5.5, 10.5 Hz, H-6″a)] corresponding to a *β*-glucose unit, in addition to two methyl singlets [δ_H 1.41 (H$_3$-1‴) and 1.52 (H$_3$-3‴)]. The ^{13}C and DEPT NMR spectra of **1** (Table 1) also exhibited signals corresponding to davidigenin and a *β*-glucose moiety, together with those of two methyls [δ_C 19.3 (C-3‴) and 29.4 (C-1‴)] and an acetal carbon [δ_C 100.9 (C-2‴)]. In the HMBC spectrum of Figure 1, correlations were observed from the two methyls to the acetal carbon, which suggested the presence of an acetonide unit. The HMBC correlation from H-6″a to the quaternary acetal carbon was consistent with the placement of the acetonide moiety as being attached to OH-4″ and -6″ of the *β*-glucose unit. The HMBC correlation from H-1″ to C-4′ (δ_C 164.8 Hz) confirmed the location of the sugar moiety at C-4′ of the davidigenin unit. The relative configuration of **1** was assigned by analyzing the coupling constants and ^{1}H−^{1}H NOESY data (Figure 2). The large coupling constant ($J_{1'',2''}$ = 7.3 Hz) suggested the *trans*-disposition of H-1″ (*α*) and H-2″ (*β*). The presence of NOESY correlations between H-1″/H-3″ and H-1″/H-5″ suggested their *α*-axial orientation, while correlations between H-4″/H-6″b indicated a *β*-axial orientation. Furthermore, NOESY correlations between H$_3$-1‴/H-4″, H$_3$-1‴/H-6″b and H-4″/H-6″b suggested the *trans*-fusion of the *β*-glucose moiety with a ring-bearing acetonide unit, with both rings adopting a chair conformation. Finally, acid hydrolysis of **1** was carried out to confirm the absolute configuration of the glucose moiety, which yielded a sugar with $[\alpha]^{25}_D$ +67.7 (*c* 0.06, H$_2$O) (Figure S11, Supporting Information), similar to the value reported for D-glucose of $[\alpha]^{25}_D$ +52 (*c* 0.02, H$_2$O).[25] Thus, the structure of **1** was assigned as davidigenin-4′-*O*-(4″,6″-*O*-isopropylidene-*β*-D-glucopyranoside).

The occurrence of an acetonide moiety among natural products is rare but does exist in Nature.[26−28] A phenylpropanoid with an acetonide unit has been reported recently from the rhizomes of *Acorus gramineus*.[29] A resocyclic acid lactone with a natural acetonide group was isolated from *Colchiobolus lunatus*.[30] However, an acetonide incorporated in a sugar unit has never been found from Nature before. Therefore, in an attempt to confirm **1** as being a natural compound, 20 mg of confusoside (**4**), which lacks the acetonide unit in **1**, was dissolved in acetone (5 mL) and allowed to stir at room temperature for 1 week. Afterward, the solvent was evaporated, and the product was subjected to ^{1}H NMR spectroscopic analysis. There was no change in the structure of confusoside (**4**). Moreover, acetone was not used throughout the extraction and isolation processes in the present phytochemical investigation. Therefore, it is proposed that fragranone A (**1**) represents the first example of a rare natural product bearing an acetonide glucose moiety.

Fragranone B (**2**) was isolated as a yellow oil. It showed a molecular ion peak at *m*/*z* 389.08816 [M + H]$^+$, corresponding to the molecular formula, $C_{19}H_{16}O_9$. The IR spectrum of **2** showed absorption bands due to hydroxy (3407 cm^{-1}) and *α*,*β*-unsaturated carbonyl (1602 cm^{-1}) groups. The

DOI: 10.1021/acs.jnatprod.9b00735
J. Nat. Prod. XXXX, XXX, XXX−XXX

Table 1. ^{1}H NMR (400 MHz) and ^{13}C NMR (100 MHz) Spectroscopic Data of 1 and 2

	1[a]		2[b]	
position	δ_H (J in Hz)	δ_C, type	δ_H (J in Hz)	δ_C, type
1		133.1, C		113.0, C
2	7.06, d (8.5)	130.4, CH	7.45, d (1.8)	117.8, CH
3	6.70, d (8.5)	116.3, CH		145.4,[d] C
4		156.7, C		147.9, C
5	6.70, d (8.5)	116.3, CH	6.84, d (8.0)	115.9, CH
6	7.06, d (8.5)	130.4, CH	7.25, dd (1.8, 8.0)	124.4, CH
α	3.23, t (7.6)	41.3, CH_2		145.5,[d] C
β	2.92, t (7.6)	30.8, CH_2	6.64, s	111.8, CH
CO		206.2, C		181.0, C
1′		116.1, C		123.3, C
2′		165.8, C		166.1, C
3′	6.56, d (2.4)	105.0, CH	6.75, d (1.8)	98.2, CH
4′		164.8, C		167.3, C
5′	6.59, dd (2.4, 9.2)	109.3, CH	6.71, dd (1.8, 8.5)	112.8, CH
6′	7.81, d (9.2)	133.5, CH	7.60, d (8.5)	125.6, CH
1″	5.09, d (7.3)	101.6, CH		
2″	3.50−3.53[e]	75.6[c], CH		175.5, C
3″	3.56−3.58[e]	74.9[c], CH	4.08, d (6.7)	72.9, CH
4″	3.58−3.6[e]	74.5[c], CH	4.15, ddd (6.7, 6.7, 6.7)	72.1, CH
5″	3.45−3.50[e]	68.7, CH	4.33, dd (6.7, 8.8) 3.85, dd (6.7, 8.8)	69.7, CH_2
6″	3.91, dd (5.5, 10.5) 3.78, dd (10.4, 10.5)	63.1, CH		
1‴	1.41, s	29.4, CH_3		
2‴		100.9, C		
3‴	1.52, s	19.3, CH_3		

[a]Measured in CD_3OD. [b]Measured in DMSO-d_6. [c]Interchangeable. [d]Interchangeable. [e]Overlapped.

UV spectrum of **2** exhibited absorption maxima at 208, 344, and 376 nm. In turn, the ^{1}H NMR spectrum of **2** (Table 1) displayed signals due to the presence of two ABX-type phenyl rings [δ_H 6.71 (dd, J = 1.8, 8.5 Hz, H-5′), 6.75 (d, J = 1.8 Hz, H-3′), 7.60 (d, J = 8.5 Hz, H-6′), 6.84 (d, J = 8.0 Hz, H-5), 7.25 (dd, J = 1.8, 8.0 Hz, H-6), and 7.45 (d, J = 1.8 Hz, H-2)] and the signals characteristic for one AMXY system [δ_H 3.85 (dd, J = 6.7, 8.8 Hz, H-5″b), 4.08 (d, J = 6.7 Hz, H-3″), 4.15 (ddd, J = 6.7, 6.7, 6.7 Hz, H-4″), and 4.33 (dd, J = 6.7, 8.8 Hz, H-5″a)]. The ^{13}C NMR spectrum of **2** (Table 1), in combination with DEPT analysis, showed the presence of 19 carbons corresponding to an oxymethylene (δ_C 69.7), two oxymethines (δ_C 72.1, 72.9), seven olefinic methines (δ_C 98.2, 111.8, 112.8, 115.9, 117.8, 124.4, 125.6), two olefinic quaternary carbons (δ_C 113.0, 123.3), five oxygenated quaternary carbons (δ_C 145.4, 145.5, 147.9, 166.1, 167.3), and two carbonyl carbons (δ_C 175.5, 181.0). Part of the ^{1}H and ^{13}C NMR data set resembled those of 3,4,2′,4′,α-pentahydroxychalcone, as confirmed from the COSY, HMQC, and HMBC spectra of **2** (Figure 1).[31]

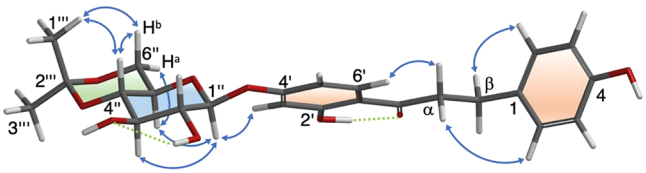

Figure 2. Most stable conformer of **1** calculated at the DFT/B3LYP/6-31G* level of theory showing hydrogen bonds (dashed blue lines) and key NOESY correlations (blue arrows) observed for **1**.

The remaining carbon signals of **2** were identified as an oxymethylene (δ_C 69.7, C-5″), two oxymethines (δ_C 72.9, C-3″ and δ_C 72.1, C-4″), and an ester carbonyl (δ_C 175.5, C-2″). In the COSY spectrum, correlations were observed between H-3″, H-4″, and H_2-5″, suggesting the connectivity between C-3″−C-4″−C-5″. In the HMBC spectrum, correlations were observed from H-3″, H-5″a, and H-5″b to an ester carbonyl carbon (C-2″), suggesting the presence of an α-hydroxy-γ-butyrolactone unit. Moreover, an HMBC correlation from H-4″ to C-4′ (δ_C 167.3) suggested an ether linkage between the lactone and the chalcone unit through C-4″−C-4′, thus establishing the planar structure of fragranone B (**2**). The relative configuration of **2** was assigned by a difference NOE experiment (Figure 3) and coupling constant data ($J_{3'',4''}$ = 6.7 Hz). Irradiation of the H-4″ (δ_H 4.15) signal caused the NOE enhancement of H-5″a (δ_H 4.33, 3.6%) without any effect on H-5″b. On the other hand, irradiation of the H-3″ (δ_H 4.08) signal caused a NOE enhancement of H-5″b (δ_H 3.85, 2.6%) without any effect on H-5″a, which suggested the relative orientation of H-3″ and H-5″b on the same side of the molecule. Therefore, the α-hydroxy-γ-butyrolactone unit in **2** was concluded to be threono-1,4-lactone. The absolute configuration of the α-hydroxy lactones can be deduced by employing the axial halo-ketone rule, with the orientation of the α-hydroxy group determined from the sign of the electronic circular dichroism (ECD) spectrum Cotton effect.[32,33] According to this rule, the S (or R) configuration at the α-carbon gives a positive (or a negative) Cotton effect at 220−230 nm. In the ECD spectrum of **2**, a negative Cotton effect was observed at 223 nm (Figure 4), suggesting the R-configuration at C-3″. Therefore, the lactone was identified as

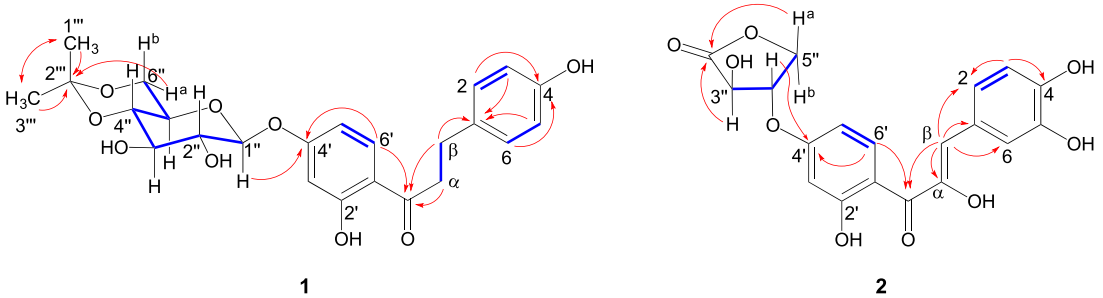

Figure 1. Connectivity (bold blue lines) deduced by COSY and HMQC and significant HMBC correlations (red arrows) in **1** and **2**.

DOI: 10.1021/acs.jnatprod.9b00735
J. Nat. Prod. XXXX, XXX, XXX−XXX

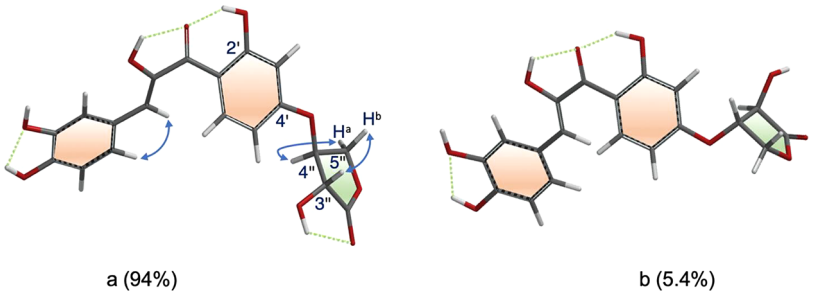

Figure 3. Most stable conformers of **2** calculated at the DFT/B3LYP/6-31G* level of theory. The relative populations are in parentheses. NOESY correlations (blue arrows) and hydrogen bonds (dashed blue lines) in **2**.

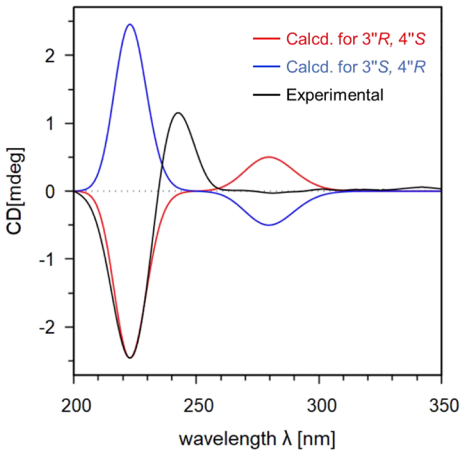

Figure 4. Experimental and calculated ECD spectra of **2**.

L-threono-1,4-lactone. The absolute configuration of **2** was further confirmed by computational ECD calculation using density functional theory (DFT). The (3″*R*,4″*S*) configuration for **2** was analyzed for the lowest energy conformation and their Boltzmann distribution, followed by optimization using DFT theory at the B3LYP/6-31+G* level. Two stable conformers with predominating relative populations, 94% and 5.4%, were obtained (Figure 3). DFT-optimized results suggested the presence of four-intramolecular hydrogen bonding in the predominating conformer "a", resulting in the most stable lowest energy state. The second stable conformer "b", however, had only three-intramolecular hydrogen bonding (Figure 3). The theoretical ECD calculations on these two optimized geometries were carried out at the same level of theory. The experimental ECD spectrum (Figure 4) matched closely with the theoretical ECD spectrum for the (3″*R*, 4″*S*) configuration, confirming the absolute configuration of **2** as 3″*R*,4″*S*. There are only a few reports for the isolation of *C*-methylated or glycosylated threonolactones from Nature.[34−36] However, this is the first report of a naturally occurring threonolactone with an ether linkage. The biogenetic formation of **2** could involve the coupling of the L-threonic acid with a 3,4,2′,4′,α-pentahydroxychalcone unit through an ether linkage followed by the lactonization of the L-threonic acid moiety to give fragranone B (**2**) (Figure 5).

All isolated compounds were tested for their preferential cytotoxic activity against the PANC-1 cell line in both nutrient-deprived medium (NDM) and standard nutrient-rich medium (Dulbecco's modified Eagle medium, DMEM), using an antiausterity strategy.[4] The data are presented as preferential cytotoxicity (PC_{50}) values, which represent the concentration of 50% cancer cell death in NDM without any toxicity in DMEM (Table 2). Among the compounds tested, betulin (**14**) displayed the most potent preferential cytotoxicity, with a PC_{50} value of 8.4 μM. Lupeol (**13**), which contains a hydroxymethylene group at C-28, showed a weaker activity (PC_{50} 38.6 μM) than betulin (**14**). In case of the flavones, the activity found was in the order **8** > **11** > **9** > **12** > **10**. Among the chalcones, the dihydrochalcone-4′-*O*-glucoside **5** and its parent

Table 2. Preferential Cytotoxicity (PC_{50}) of Compounds 1−17 against the PANC-1 Human Pancreatic Cancer Cell Line in Nutrient-Deprived Medium (NDM)[a]

compound	PC_{50}, μM[a]	compound	PC_{50}, μM[a]
1	60.9	**10**	>100
2	>100	**11**	17.4
3	10.5	**12**	67.1
4	82.6	**13**	38.6
5	10.4	**14**	8.4
6	>100	**15**	58.1
7	67.0	**16**	14.7
8	8.9	**17**	26.9
9	21.8	arctigenin[b]	0.7

[a]Concentration at which 50% of cells were killed preferentially in NDM. [b]Positive control.

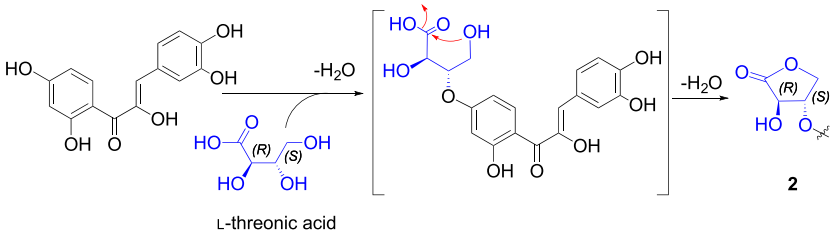

Figure 5. Plausible biogenetic pathway for **2**.

DOI: 10.1021/acs.jnatprod.9b00735
J. Nat. Prod. XXXX, XXX, XXX−XXX

aglycone **3** showed PC_{50} values of 10.4 and 10.5 μM, respectively.

During the development of pancreatic cancer, the primary tumor mass engineers migratory cells that can invade adjacent tissues and circulate to distant organs where cancer cells have sufficient nutrients to grow and form new colonies. These processes are responsible for ~90% of pancreatic cancer deaths in patients.[37] Thus, finding inhibitors of pancreatic cancer cell migration is crucial for suppressing the process of pancreatic tumor metastasis. The uniqueness of the structure of **1** in addition to its noncytotoxicity under nutrient-rich conditions encouraged an evaluation of the ability of **1** to inhibit PANC-1 cell migration using a quantitative real-time cell migration assay. Fragranone A (**1**) was exposed to PANC-1 cells in a standard nutrient-rich medium (DMEM) against the monolayer of PANC-1 cell scratch. Parallel experiments were run under the same culture conditions for the control and the treated cells, and the real-time images were captured every 15 min for 72 h automatically through a digital microscope installed within a CO_2 incubator (Figure 6A).

Altogether, 319 images were captured for each group (Figure S23, Supporting Information). The wound area at each interval of time was quantified using a Fiji platform.[38] Compound **1** was found to inhibit PANC-1 cell migration in real time compared to the control (Movie 1, Supporting Information). The velocity of migration in the control PANC-1 cells was found to be quite fast compared to the treated group, and the wound area was closed to 38% within 24 h when compared to the initial wound at 0 h (100%). PANC-1 cells treated with fragranone A (**1**), on the other hand, led to significant inhibition of migration, so that the wound area remained open to 93% after 24 h. This difference was reduced at 48 h, and the gap of the wound area was found to be 12% and 81% for the control and the treated group, respectively. After 72 h, less than 5% of the wound area remained in the control, while the treated cells still had a 72% open wound area (Figure 6B). These results suggested that fragranone A (**1**) has the ability to suppress the migration of PANC-1 cells. This real-time cancer cell migration inhibition study has a significant benefit over conventional end-point measurement in a migration assay in several aspects. Conventional methods are often subjective, and the length of the measured wound may vary due to differences in the exact photographic location. Since cancer cell migration is heterogeneous, conventional end point measurement of a wound length often leads to inaccuracy, as the length of the wound at different locations might be different. Real-time wound areas address the issue of heterogeneous cancer cell migration and provide reliable quantitative information in real time without any bias, because the wound study area remains fixed throughout the study period within the CO_2 incubator without any external disturbances.

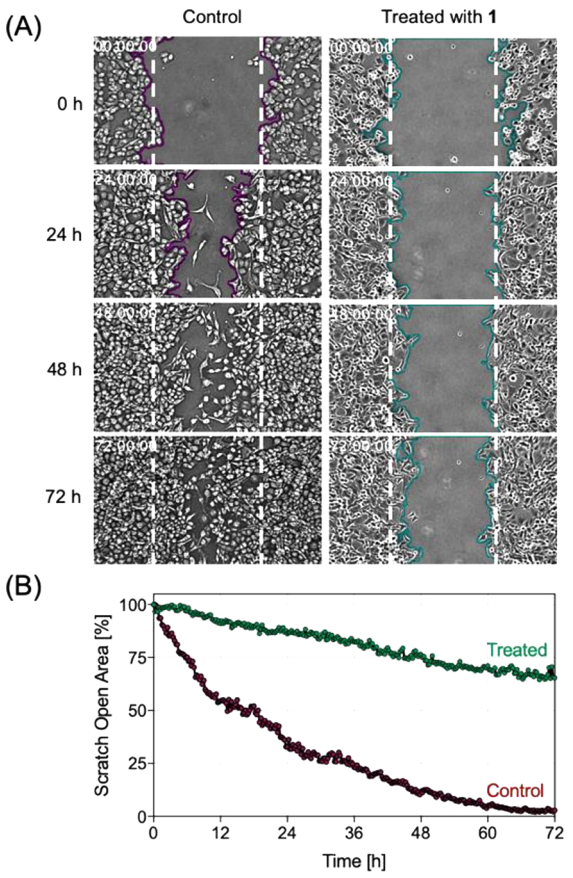

Figure 6. Fragranone A (**1**) suppresses the migration of PANC-1 cells in a wound-healing assay in real time. (A) The white lines indicate the wound length at the start of the experiment. Treated and control cells were subjected to time-lapse imaging at 15 min intervals for 72 h, and the representative images are shown. (B) Quantification of wound healing by measuring the open scratch area for each time point.

EXPERIMENTAL SECTION

General Experimental Procedures. Optical rotations and ECD spectra were measured on a JASCO P-2100 digital polarimeter and a JASCO J-805 spectropolarimeter, respectively. UV spectra were recorded on a U-5100 UV−visible ratio-beam spectrophotometer (Hitachi). IR spectra were measured with a JASCO FT/IR-460 Plus spectrophotometer. NMR spectra were recorded using a JEOL ECX400 Delta spectrometer with tetramethylsilane as internal standard, and chemical shifts are expressed in δ values. HRFABMS measurements were carried out on a JEOL JMS-AX505HAD mass spectrometer. Medium-pressure liquid chromatography (MPLC) was performed with a Büchi MPLC C-605 dual-gradient pump system using normal-phase silica gel (silica gel 60N, spherical, neutral, 40−50 μm) purchased from Kanto Chemical, Japan. Analytical and preparative thin-layer chromatography (TLC) were carried out on precoated silica gel 60F254 and RP-18F254s plates (0.25 or 0.50 mm, Merck KGaA, Darmstadt, Germany) and precoated silica gel 70 PF254 plates (0.75 mm thickness) from Wako (Wako Pure Chemical Industries, Ltd., Japan).

Plant Material. Leaves of *A. fragrans* were collected at Omkoi district, Chiang Mai Province, Thailand, on November 2017. The plant material was identified by Mr. Wittaya Pongamornkul, and a voucher specimen (NDD2017-AFL) has been deposited in the Natural Drug Discovery Laboratory, University of Toyama, Japan.

Extraction and Isolation. Air-dried leaves (1 kg) of *A. fragrans* were ground to a fine powder, which was then extracted with 95% EtOH in three cycles (3 days/cycle) at room temperature. The extracts were combined and concentrated under reduced pressure to yield an ethanolic extract (105 g). The extract (100 g) was suspended in H_2O (200 mL) and partitioned successively with CH_2Cl_2 (4 × 200 mL) and EtOAc (4 × 200 mL) to give CH_2Cl_2 (5.4 g), EtOAc (17.3 g), and H_2O (74 g) soluble fractions, respectively. The EtOAc-soluble fraction was subjected to silica gel column chromatography using an *n*-hexane−EtOAc gradient mixture (0−100%) followed by an EtOAc−MeOH gradient system (0−100%) to give 12 fractions (Fr. 1, 3.6 g; Fr. 2, 847 mg; Fr. 3, 322 mg; Fr. 4, 110 mg; Fr. 5, 900 mg; Fr. 6, 1.2 g; Fr. 7, 215 mg; Fr. 8, 120 mg; Fr. 9, 490 mg; Fr. 10, 310 mg; Fr. 11, 8.9 g; Fr. 12, 460 mg). Fraction 2 (847 mg) was washed with

DOI: 10.1021/acs.jnatprod.9b00735
J. Nat. Prod. XXXX, XXX, XXX−XXX

n-hexane to obtain lupeol (**13**, 396 mg). Fraction 4 (110 mg) was rechromatographed on silica gel by MPLC using an *n*-hexane−EtOAc gradient system (0−100%) to give spinasterol (**15**, 1 mg). Fraction 5 (900 mg) was recrystallized from an *n*-hexane−EtOAc solvent mixture to give betulin needles (**14**, 42 mg). Fraction 7 (215 mg) was purified by normal-phase MPLC using a CH_2Cl_2−MeOH gradient system (0−100%) to yield 3,4,2′,4′-tetrahydroxydihydrochalcone (**3**, 154 mg). Fraction 8 (120 mg) was rechromatographed on silica gel using MPLC with a CH_2Cl_2−MeOH gradient mixture (0−100%) followed by preparative TLC with a CH_2Cl_2−MeOH solvent mixture (97:3) to give butein (**7**, 0.9 mg). Fraction 9 (490 mg) was also rechromatographed on silica gel by MPLC using a CH_2Cl_2−MeOH gradient system (0−100%) to give five subfractions (Fr. 9-1, 11 mg; Fr. 9-2, 12 mg; Fr. 9-3, 116 mg; Fr. 9-4, 14 mg; Fr. 9-5, 189 mg). Subfraction 9-4 was obtained as pure fragranone B (**2**, 14 mg). Subfraction 9-2 (12 mg) was purified by preparative TLC with a CH_2Cl_2−MeOH solvent mixture (98:2) to yield isoscopoletin (**17**, 0.6 mg). Subfraction 9-5 (189 mg) was further purified by preparative TLC with CH_2Cl_2−MeOH solvent mixture (85:15) to give a mixture of (+)-catechin and (−)-epicatechin (**16**, 36 mg). Fraction 11 (8.9 g) was rechromatographed on RP-silica gel with MPLC using an eluent system consisting of solvent A [H_2O] and solvent B [CH_3CN−MeOH (1:1)], with a gradient (0−100% B) to give seven subfractions (Fr. 11-1, 205 mg; Fr. 11-2, 411 mg; Fr. 11-3, 3.2 g; Fr. 11-4, 4.5 g; Fr. 11-5, 199 mg; Fr. 11-6, 30 mg; Fr. 11-7, 335 mg). Subfraction 11-2 (411 mg) was rechromatographed on silica gel by MPLC using an EtOAc−MeOH gradient system (0−100%) followed by preparative TLC with an EtOAc−MeOH solvent mixture (9:1) to give davidioside (**6**, 60 mg), isoquercetrin (**10**, 4.7 mg), and kaempferol 3-neohesperidoside (**11**, 16 mg). Subfraction 11-3 (3.2 g) was rechromatographed on silica gel with MPLC using an EtOAc−MeOH gradient system (0−100%) to give four subfractions (Fr. 11-3-1, 5 mg; Fr. 11-3-2, 347 mg; Fr.11-3-3, 1.2 g; Fr.11-3-4, 123 mg). Subfractions 11-3-1 and 11-3-3 were identified as quercetrin (**9**, 5 mg) and vacciniifolin (**5**, 1.2 g), respectively. Subfraction 11-3-4 (123 mg) was further chromatographed on silica gel with MPLC using a CH_2Cl_2−MeOH gradient system (0−100%) to afford nictoflorin (**12**, 25 mg). Subfraction 11-4 (3.9 g) was rechromatographed on silica gel by MPLC using an EtOAc−MeOH gradient system (0−100%) followed by preparative TLC with an EtOAc−MeOH solvent mixture (9:1) to produce confusoside (**4**, 3.3 g) and afzelin (**8**, 27 mg). Subfraction 11-6 (30 mg) was further purified by preparative TLC with an EtOAc−MeOH solvent mixture (98:2), which afforded fragranone A (**1**, 5.5 mg).

*Fragranone A (**1**):* white, amorphous powder; $[\alpha]^{25}_D$ −15 (*c* 0.03, MeOH); UV (MeOH) λ_{max} (log ε) 208 (4.24), 272 (3.84), 320 (3.51) nm; IR (KBr) ν_{max} 3420, 1634 cm^{-1}; ^1H NMR (400 MHz, CD_3OD) and ^{13}C NMR (100 MHz, CD_3OD) data, see Table 1; HRFABMS *m*/*z* 461.18126 $[M + H]^+$ (calcd for $C_{24}H_{28}O_9$, 461.18113).

*Fragranone B (**2**):* yellow oil; $[\alpha]^{25}_D$ +136.8 (*c* 0.1, MeOH); UV (MeOH) λ_{max} (log ε) 208 (5.07), 344 (4.48), 376 (4.55) nm; ECD (*c* 2.6×10^{-4} M, EtOH) λ_{max} ($\Delta\varepsilon$) 223 (−2.5), 242 (+1.8); IR (KBr) ν_{max}3407, 1602 cm^{-1}; ^1H NMR (400 MHz, DMSO-d_6) and ^{13}C NMR (100 MHz, DMSO-d_6) data, see Table 1; HRFABMS *m*/*z* 389.08816 $[M + H]^+$ (calcd for $C_{19}H_{16}O_9$, 389.08723).

Acid Hydrolysis of 1. Fragranone A (**1**, 1.9 mg) was heated with 6% HCl (1 mL) for 5 h at 80 °C. The reaction mixture was extracted with CH_2Cl_2 (4 × 3 mL), and the aqueous phase was dried by using a Genevac EZ-2 vacuum centrifuge. The resulting residue (4.2 mg) was purified by preparative TLC with a CH_2Cl_2−MeOH−H_2O solvent mixture (8:5:1) to yield glucose (0.7 mg), $[\alpha]^{25}_D$ +67.7 (*c* 0.06, H_2O). Identification of glucose was done through ^1H NMR spectroscopic analysis (Figure S11, Supporting Information).[39]

ECD Calculations for 2. The conformational search was performed on Spartan'14 by using the MMFF molecular force field.[40] Eight conformers with a Boltzmann distribution were reoptimized using DFT at the B3LYP/6-31+G* level in the gas phase, which suggested two predominant conformers having a relative population of 94% and 5.4%. The theoretical ECD calculations on these optimized geometries were carried out at the same level of theory in a PCM solvation model for EtOH in Gaussian 09.[41] The output files were summed to obtain Boltzmann-weighted spectra and compared with the experimental spectra using SpecDis v. 1.71. A UV correction (−18 nm) was carried out with respect to the experimental value.[42]

Preferential Cytotoxicity Assay against PANC-1 Cells. Preferential cytotoxicity of the 95% EtOH extract of *A. fragrans* and the isolated compounds was determined by a procedure described previously.[4]

Quantitative Real-Time Cell Migration Assay. PANC-1 cells (9×10^6 cells/well) were seeded in a 35 mm Petri dish and allowed to attach for 24 h. The monolayers were then incised with a micropipet tip in the central area of the culture to create a wound.

Cells were then treated with either DMEM alone (the control) or DMEM containing fragranone A (**1**, 100 μM) and placed on the CytoSMART systems installed within a CO_2 incubator. The images were captured every 15 min automatically. The open wound area in each image was calculated using Fiji software, and the data were processed using GraphPad Prism 7.

■ ASSOCIATED CONTENT

Supporting Information

The Supporting Information is available free of charge on the ACS Publications website at DOI: 10.1021/acs.jnatprod.9b00735.

Copies of spectroscopic data for **1** and **2** (PDF)

Captures of live imaging of real-time cell migration assay (PDF)

Real-time movie showing the inhibitory effect of fragranone A (**1**, 100 μM) on the migration of PANC-1 cells (AVI)

■ AUTHOR INFORMATION

Corresponding Author

*Tel: +81-76-434-7640. Fax: +81-76-434-7640. E-mail (S. Awale): suresh@inm.u-toyama.ac.jp.

ORCID

Suresh Awale: 0000-0002-5299-193X

Notes

The authors declare no competing financial interest.

■ ACKNOWLEDGMENTS

This work was supported by the Japanese Society for the Promotion of Science (JSPS), Japan, Kakenhi (16K08319), and Kobayashi International Scholarship to S.A. The authors thank the Egyptian-Japanese Education partnership (EJEP) fellowship for supporting A.M.O. and A.M.T.

■ REFERENCES

(1) Bray, F.; Ferlay, J.; Soerjomataram, I.; Siegel, R. L.; Torre, L. A.; Jemal, A. *Ca-Cancer J. Clin.* **2018**, *68*, 394−424.

(2) The Editorial Board of Cancer Statistics in Japan. *Cancer Statistics in Japan 2018*; Foundation for Promotion of Cancer Research (FPCR), 2018. http://ganjoho.jp/en/professional/statistics/brochure/index.html.

(3) Poruk, K. E.; Firpo, M. A.; Adler, D. G.; Mulvihill, S. J. *Ann. Surg.* **2013**, *257*, 17−26.

(4) Awale, S.; Lu, J.; Kalauni, S. K.; Kurashima, Y.; Tezuka, Y.; Kadota, S.; Esumi, H. *Cancer Res.* **2006**, *66*, 1751−1757.

(5) (a) Izuishi, K.; Kato, K.; Ogura, T.; Kinoshita, T.; Esumi, H. *Cancer Res.* **2000**, *60*, 6201−6207. (b) Lu, J.; Kunimoto, S.; Yamazaki, Y.; Kaminishi, M.; Esumi, H. *Cancer Sci.* **2004**, *95*, 547−552. (c) Esumi, H.; Lu, J.; Kurashima, Y.; Hanaoka, T. *Cancer Sci.* **2004**, *95*, 685−690.

DOI: 10.1021/acs.jnatprod.9b00735
J. Nat. Prod. XXXX, XXX, XXX−XXX

(6) Awale, S.; Nakashima, E.M. N.; Kalauni, S. K.; Tezuka, Y.; Kurashima, Y.; Lu, J.; Esumi, H.; Kadota, S. *Bioorg. Med. Chem. Lett.* **2006**, *16*, 581−583.
(7) Nguyen, N. T.; Nguyen, M. T. T.; Nguyen, H. X.; Dang, P. H.; Dibwe, D. F.; Esumi, H.; Awale, S. *J. Nat. Prod.* **2017**, *80*, 141−148.
(8) Sun, S.; Phrutivorapongkul, A.; Dibwe, D. F.; Balachandran, C.; Awale, S. *J. Nat. Prod.* **2018**, *81*, 1877−1883.
(9) Awale, S.; Dibwe, D. F.; Balachandran, C.; Fayez, S.; Feineis, D.; Lombe, B. K.; Bringmann, G. *J. Nat. Prod.* **2018**, *81*, 2282−2291.
(10) Siddaiah, V.; Rao, C. V.; Venkateswarlu, S.; Subbaraju, G. V. *Tetrahedron* **2006**, *62*, 841−846.
(11) Tanaka, T.; Kawamura, K.; Kohda, H.; Yamasaki, K.; Tanaka, O. *Chem. Pharm. Bull.* **1982**, *30*, 2421−2423.
(12) Ling, T. J.; Lin, L. D.; Wu, P.; Zhou, W. H.; Ye, H. G.; Liu, M. F.; Wei, X. Y. *Chin. Chem. Lett.* **2004**, *15*, 1182−1184.
(13) Gutmann, A.; Bungaruang, L.; Weber, H.; Leypold, M.; Breinbauer, R.; Nidetzky, B. *Green Chem.* **2014**, *16*, 4417−4425.
(14) Junior, G. M. V.; de M. Sousa, C. M.; Cavalheiro, A. J.; Lago, J. H. G.; Chaves, M. H. *Helv. Chim. Acta* **2008**, *91*, 2159−2167.
(15) Chen, C.-Y.; Hsieh, S.-L.; Hsieh, M.-M.; Hsieh, S.-F.; Hsieh, T.-J. *Chin. Pharm. J.* **2004**, *56*, 141−146.
(16) Aderogba, M. A.; Kgatle, D. T.; McGaw, L. J.; Eloff, J. N. *S. Afr. J. Bot.* **2012**, *79*, 125−131.
(17) Han, J.-T.; Bang, M.-H.; Chun, O.-K.; Kim, D.-O.; Lee, C.-Y.; Baek, N.-I. *Arch. Pharmacal Res.* **2004**, *27*, 390−395.
(18) Kazuma, K.; Noda, N.; Suzuki, M. *Phytochemistry* **2003**, *62*, 229−237.
(19) Park, S. Y.; Kim, J. S.; Lee, S. Y.; Bae, K.; Kang, S. S. *Nat. Prod. Sci.* **2008**, *14*, 281−288.
(20) Mahato, S. B.; Kundu, A. P. *Phytochemistry* **1994**, *37*, 1517−1575.
(21) Iida, T.; Ishikawa, T.; Tamura, T.; Matsumoto, T. *J. Japan Oil Chem. Soc.* **1980**, *29*, 345−346.
(22) Galotta, A. L. Q. A.; Boaventura, M. A. D.; Lima, L. A. R. S. *Quim. Nova* **2008**, *31*, 1427−1430.
(23) Zhao, D.-D.; Zhao, Q.-S.; Liu, L.; Chen, Z.-Q.; Zeng, W.-M.; Lei, H.; Zhang, Y.-L. *Molecules* **2014**, *19*, 3345−3355.
(24) Desire, O.; Rivière, C.; Razafindrazaka, R.; Goossens, L.; Moreau, S.; Guillon, J.; Uverg-Ratsimamanga, S.; Andriamadio, P.; Moore, N.; Randriantsoa, A.; Raharisololalao, A. *J. Ethnopharmacol.* **2010**, *130*, 320−328.
(25) Kim, K. H.; Park, Y. J.; Chung, K. H.; Yip, M. R.; Clardy, J.; Senger, D.; Cao, S. *J. Nat. Prod.* **2015**, *78*, 320−324.
(26) Arriaga, F. J.; Rumbero, A.; Wollenweber, E. *Z. Naturforsch., C: J. Biosci.* **1996**, *51*, 423−425.
(27) Mamadalieva, N. Z.; Janibekov, A. A.; Girault, J.-P.; Lafont, R. *Nat. Prod. Commun.* **2010**, *5*, 1579−1582.
(28) Yamaguchi, I.; Yokota, T.; Murofushi, N.; Takahashi, N.; Ogawa, Y. *Agric. Biol. Chem.* **1975**, *39*, 2399−2403.
(29) Yu, J. S.; Moon, E.; Choi, S. U.; Kim, K. H. *Tetrahedron Lett.* **2016**, *57*, 1699−1701.
(30) Shao, C. L.; Wu, H. X.; Wang, C. Y.; Liu, Q. A.; Xu, Y.; Wei, M. Y.; Qian, P. Y.; Gu, Y. C.; Zheng, C. J.; She, Z. G.; Lin, Y. C. *J. Nat. Prod.* **2011**, *74*, 629−633.
(31) Metuno, R.; Ngandeu, F.; Tchinda, A. T.; Ngameni, B.; Kapche, G. D. W.F.; Djemgou, P. C.; Ngadjui, B. T.; Bezabih, M.; Abegaz, B. M. *Biochem. Syst. Ecol.* **2008**, *36*, 148−152.
(32) Meguro, H.; Konno, T.; Tuzimura, K. *Agric. Biol. Chem.* **1973**, *37*, 945−947.
(33) Nakaminami, G.; Edo, H.; Nakagawa, M. *Bull. Chem. Soc. Jpn.* **1973**, *46*, 266−269.
(34) Syed, A. S.; Akram, M.; Bae, O.-N.; Kim, C. Y. *Chem. Nat. Compd.* **2019**, *55*, 8−10.
(35) Uriburu, M. L.; Gil, R. R.; Sosa, V. E.; de la Fuente, J. R. *J. Arg. Chem. Soc.* **2008**, *96*, 55−61.
(36) Lee, C.-L.; Huang, P.-C.; Hsieh, P.-W.; Hwang, T.-L.; Hou, Y.-Y.; Chang, F.-R.; Wu, Y.-C. *Planta Med.* **2008**, *74*, 1276−1279.
(37) Keleg, S.; Büchler, P.; Ludwig, R.; Büchler, M. W.; Friess, H. *Mol. Cancer* **2003**, *2*, 1−7.
(38) Schindelin, J.; Arganda-Carreras, I.; Frise, E.; Kaynig, V.; Longair, M.; Pietzsch, T.; Preibisch, S.; Rueden, C.; Saalfeld, S.; Schmid, B.; Tinevez, J.-Y.; White, D. J.; Hartenstein, V.; Eliceiri, K.; Tomancak, P.; Cardona, A. *Nat. Methods* **2012**, *9*, 676−682.
(39) Gurst, J. E. K. *J. Chem. Educ.* **1991**, *68*, 1003−1004.
(40) *SPARTAN'14*; Wavefunction: Irvine, CA, 2014.
(41) Frisch, M. J., Trucks, G. W., Schlegel, H. B., Scuseria, G. E., Robb, M. A., Cheeseman, J. R., Scalmani, G., Barone, V., Mennucci, B., Petersson, G. A., Nakatsuji, H.; Caricato, M.; Li, X.; Hratchian, H. P.; Izmaylov, A. F.; Bloino, J.; Zheng, G.; Sonnenberg, J. L.; Hada, M.; Ehara, M.; Toyota, K.; Fukuda, R.; Hasegawa, J.; Ishida, M.; Nakajima, T.; Honda, Y.; Kitao, O.; Nakai, H.; Vreven, T.; Montgomery, J. A., Jr.; Peralta, J. E.; Ogliaro, F.; Bearpark, M.; Heyd, J. J.; Brothers, E.; Kudin, K. N.; Staroverov, V. N.; Kobayashi, R.; Normand, J.; Raghavachari, K.; Rendell, A.; Burant, J. C.; Iyengar, S. S.; Tomasi, J.; Cossi, M.; Rega, N.; Millam, J. M.; Klene, M.; Knox, J. E.; Cross, J. B.; Bakken, V.; Adamo, C.; Jaramillo, J.; Gomperts, R.; Stratmann, R. E.; Yazyev, O.; Austin, A. J.; Cammi, R.; Pomelli, C.; Ochterski, J. W.; Martin, R. L.; Morokuma, K.; Zakrzewski, V. G.; Voth, G. A.; Salvador, P.; Dannenberg, J. J.; Dapprich, S.; Daniels, A. D.; Farkas, O.; Foresman, J. B.; Ortiz, J. V.; Cioslowski, J.; Fox, D. J. *Gaussian 09w (version 7.0)*; Gaussian, Inc: Wallingford, CT, 2009.
(42) Bruhn, T.; Schaumlöffel, A.; Hemberger, Y.; Pescitelli, G. *SpecDis* version 1.71; Berlin, Germany, 2017.

DOI: 10.1021/acs.jnatprod.9b00735
J. Nat. Prod. XXXX, XXX, XXX−XXX